Experimental Investigation of Influence of Vegetation on Flow Turbulence

Nazanin Mohammadzade Miyab[1], Hossein Afzalimehr[1,*], Vijay P. Singh[2]

[1]Department of water engineering, Isfahan University of Technology, Isfahan, Iran
[2]Department of Civil and Environmental Engineering, Dept. of Biological and Agricultural Engineering, Texas A&M University, USA

Abstract   Vegetation in channels, rivers, reservoirs, and wetlands alters the flow turbulence characteristics. Vegetation has both positive and negative effects, depending on the objective of the hydraulic conduit. For example, it decreases conveyance capacity by obstructing flow by reducing the flow cross-sectional area and increasing resistance to flow and may, hence, increase flooding. On the other hand, it increases bank stability, reduces erosion and turbidity, provides habitat for aquatic and terrestrial wildlife, presents aesthetic properties, and filters pollutants. Using both field and laboratory experiments, this study investigates the influence of vegetation on turbulent characteristics and flow resistance for a channel with gravel bed and vegetation on banks. The results shows that vegetation affects the velocity distribution, the position of dip phonemenon, turbulent kinematic energy and drag coefficient. These changes can be observed in the distribution of shear stress, the quadrant analysis events and statistics moments.

Keywords   Ecosystem, Gravel bed channels, Flow resistance, Turbulence, Vegetation

1. Introduction

Vegetation growing in waterways and rivers increase turbulence. As part of ecosystems, it provides habitat for animals by creating low-flow regions [1] and improves water quality by producing oxygen and removing excess nutrients [2, 3]. It consumes a great deal of energy and current momentum along the course of rivers and floodplains [4]. Momentum transfer causes shear stress on the walls, which influences the discharge of the main channel as well as of floodplains and also the erosion and sustainability of banks and the general transfer of sediments [5].

Vegetation is known to increase bank stability, reduce erosion and turbidity, provide habitat for aquatic and terrestrial wildlife, attenuate floods, present aesthetic properties, and filter pollutants [6]. Aquatic vegetation planting and management are commonly used approaches in river ecological restoration in recent years [7]. Vegetation has traditionally been viewed as an obstruction to channel flow by decreasing carrying capacity and by increasing flow resistance and the risk of flooding. In recent years, vegetation has become a major component of erosion control and stream restoration [8].

The mechanism of turbulence in channels with vegetation is of considerable importance [9], especially in mountainous regions where the dominant flow regiment in rivers is turbulent flow. This is the specific feature of Iranian rivers. Flow is termed turbulent when flow characteristics are variant and the acceleration force is much stronger than the viscous force. The exclusivity of turbulence is eddy and turbulent streams exhibit 3D temporal and spatial fluctuations. For estimating surface flooding and improving flow conditions, information on flow-vegetation interaction is important. Therefore, the objective of this study is to investigate, using both laboratory and field experiments, the influence of vegetation on turbulent characteristics and flow resistance for a channel with gravel bed and vegetation on banks.

2. Methods and Materials

In this study, both field and laboratory experiments were conducted.

Laboratory Experimentation

Flume

An experimental channel, located in the Hydraulics Laboratory at Isfahan University of Technology, was used for experimentation. The channel is rectangular in cross-section, 8 m long, 40 cm wide, and 60 cm deep. The channel wall and floor are made up of clear Plexiglas. The flow discharge and depth used were equal to 40 liters/s and an average of 15 cm, respectively.

Laboratory Experiments

Experiments were conducted in 4 series, including 2 series

with and without vegetation in which the bed slope was chosen as 0.5%, and 2 series with and without vegetation with a bed slope of 1.5%. A total of 40 velocity profiles were measured. For each profile, the point velocity was also calculated at 20-25 points along the depth of flow.

In order to keep measurements in order, it was found appropriate to use the following nomenclature. If there was vegetation then letter R (Rice) and if there was no vegetation then letter B (Bare bank) were used at the beginning of the profile and then were used the distance from the central axis in centimeter and the distance from the beginning of the channel in meter and the slope of the channel bed, respectively. For example, B0-6.5-0.5% indicates bare bank with a slope of 0.5% and the distance of 6.5 meters from beginning of channel in central axis.

To investigate the development of flow, the fourth series of experiments measured profiles in the central axis that had 5, 5.75 and 6.5 m distance from the beginning of channel, as shown in figure 1. The figure 1 shows that the distance of 5 m from the entrance of the channel is suitable to verify the fully developed flow condition where the velocity distributions are auto-similar.
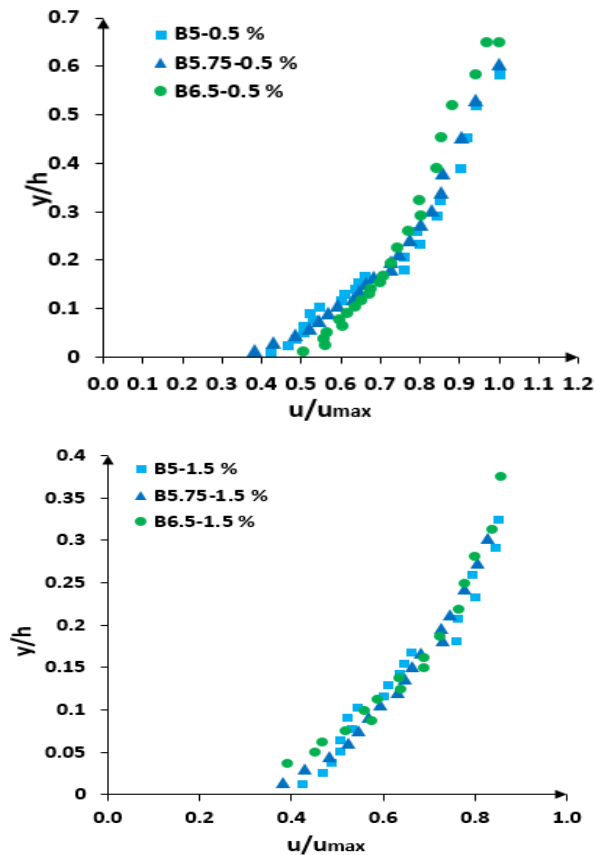

Figure 1. Development of flow in channel

Velocity meter

To measure the instantaneous velocity, the three dimensional velocity meter ADV was used. The device was set to 200Hz and the time was adjusted for 2 min based on which the speed of $200 \times 120 = 24000$ at every point of the profile was measured.

Channel bed

Gravel was chosen as a cover for the bed. In this experiment, $d_{50} = 25$ mm was selected. The flow was decelerating. The bed slope was chosen, based on previous studies and the channel conditions, such as the length and depth of the flume. In this study, two slopes of 0.5% and 1.5% were used.

Vegetation

The vegetation that was used in the experimental setup was rice with 4.2 mm stem diameter and 0.38 m height. The rice stem density was 290 stems per meter long. Figure 2 displays the experimental channel with gravel bed and vegetation on the banks.

Figure 2. Gravel bed and vegetation in bank

Field Experimentation

Selected River reach

A reach of the Babolrod River was selected. This river is one of the northern rivers in Iran and is located in the western Daronkola region in Mazandaran province. The river has a length of 110 km and the selected reach was 250 m in a straight course. The hydraulic features of the river are shown in table 1.

Table 1. Hydraulic characteristics of river

Property	Minimum	Maximum	Average
Flow depth (m)	0.14	0.65	0.36
Sections width (m)	19	25.5	22
Aspect ratio	31	97	64.5
Flow discharge (m^3/s)	1	11	4.5

The selected river section had vegetation on its left as well as right banks. The reach had 13 measured cross sections where 11 cross sections were with vegetation on banks and 2 cross sections were with bare banks. At each cross section, five velocity profiles were measured: one velocity profile at

the central part of the reach, two velocity profiles along each river bank, and two velocity profiles between the central axis of the reach and river banks. In naming the profiles, the first term was the name of the section and then the distance from the central axis in meter was given. The left and the right banks were shown by L and R. When the cross section was beside the vegetation, it was also given, as shown in figure 3. For example, A_0 suggested section A and the profile was measured in the central axis. For example, D10-LV indicates section D and the profile beside the left bank vegetation with 10 meters away from the central axis. By feeding the topography data into the software Surfer, the topography and post-maps of the cross section and the total study reach were drawn as follows:
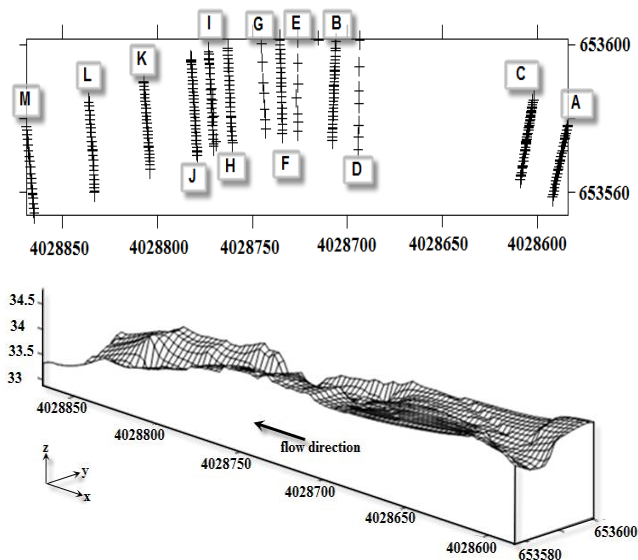

Figure 3.   Topography and post-maps display of the study reach

Velocity measurement

A butterfly current-meter was used to measure the velocity. Each point velocity measurement was taken during 50 seconds with three repetitions to get an accurate average velocity. Considering the flow depth, a range of 10-15 point velocity measurements was taken for each profile. Using the calibrated formula of the velocity meter, the points measured were converted into meters per second. The limitation of the butterfly current-meter is due to its 3 cm butterfly radius that prevents the measurement of points 3 cm away from the bed and water surface.

Topography device

A total station device and a scale were used to measure the point coordinates. First, the selected sections were marked by ropes. The points measured by the total device had parameters including X, Y and Z. X was in the direction of flow, Y in the direction of the width, and Z was in the vertical direction-along height. The measurement started from the beginning of the section and continued by one meter in a row to the end of the section. The points were fed into the software Arc GIS and calculations were made. Wherever the velocity profile was measured, the point coordinates were

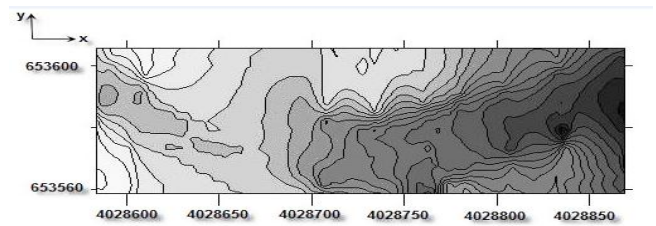measured as well. Figure 4 Indicates the contour lines measured.

Figure 4.   Display contour line of selected reach

Vegetation

According to the objective of the project, it was necessary to select a reach that had the same vegetation on the banks. For the specifications mentioned above, Western Daronkola in Mazandaran was selected. The selected reach had vegetation similar to rice on the left and right banks. This plant is flexible and emergent. The vegetation had an average height of 0.19 m and a width of 0.8 m in the area that was covered by vegetation. The vegetation that was in field setup had 3.8 mm stem diameter and rice stems density was 331 stems per meter long.

Figure 5.   Display of vegetation in banks in selected reach of Babolrod River

Bed material

Table 2 shows the characteristics of particle size in the selected reach of Babolrod River. These characteristics were obtained by average values for 13 measured cross sections. The measured reach in the Babolrod had $d_{50} = 30.58$ mm and the uniformity coefficient of the reach $(\frac{d_{60}}{d_{10}})$ Cu = 2.05 which is suggestive of the particle uniformity. Also, the average geometric measure D_g, geometric scale deviancy δ_g and gravel coefficient Gr were included, as shown in table 2.

Table 2. The characteristics of particle size

d_{50} (mm)	C_u	D_g	δ_g	Gr
30.58	2.05	31	1.64	1.65

Measured hydraulic characteristics are presented in table 3.

Table 3. Summary of hydraulic characteristics in the study reach

Section	w(m)	h (m)	$\frac{w}{h}$	A (m²)	A_p (m²)	P (m)	R	Q ($\frac{m^3}{s}$)	Re (×10⁵)	Fr	S_f (×10⁻⁴)
A	16.2	0.51	8.2	6.4	-	16.26	0.4	1.5	1.1	0.11	1.9
B	25.6	0.3	99	7.1	-	25.7	0.28	0.96	2.5	0.06	6.9
C	19	0.49	43.4	8.5	0.13	19.18	0.45	10.94	1.1	0.1	12
D	21.3	0.44	52.3	8.4	0.28	21.47	0.39	6.23	3.4	0.38	2.4
E	21.6	0.38	65.5	5.4	0.13	22.63	0.24	3.08	2.3	0.27	4.3
F	21.7	0.38	67.4	5.9	0.09	21.72	0.28	3.89	2.7	0.33	3.3
G	24.4	0.29	93.6	6.3	0.1	24.41	0.26	3.48	1.8	0.32	5.9
H	24.5	0.38	77.8	6.9	0.6	25.52	0.27	7.73	4.3	0.59	12
I	24.4	0.36	70.4	6.4	0.21	25.46	0.25	7.25	4.1	0.6	8
J	24.5	0.34	74	5.1	0.21	24.57	0.21	4.95	3.4	0.53	9.8
K	22.2	0.31	71.4	6.1	0.16	22.38	0.27	5.44	0.7	0.01	8
L	22	0.36	72.3	3.3	0.28	22.06	0.15	1.34	1.4	0.24	3
M	22.4	0.23	97	2.1	0.07	22.42	0.09	1.12	1.9	0.48	9.5

Background and method of calculation

Flow condition

Reynolds numbers and Froude numbers were used for the determination of the basic flow condition:

$$Re = \frac{\rho u R}{\mu} \tag{1}$$

$$Fr = \frac{u}{\sqrt{gh}} \tag{2}$$

Where u is the main flow velocity ($\frac{m}{s}$), R is the hydraulic radius (m), μ is the dynamic viscosity (Pa.s), h is the water depth (m), and g is the gravitational acceleration.

According to table 3 in the field case, since the Reynolds number was 2×10^5 the flow was unsteady and Froude number was 0.3 which indicated subcritical flow.

The Reynolds number was from 12.5×10^5 to 6×10^4 for the laboratory experiments. This indicated that the flow regime can be considered as turbulent flow. The flow was subcritical because the Froude number was less than 1 for all laboratory experiments.

Colosimu et al. [10] and Afzalimehr and Anctil [11] introduced the Shields parameter as one of the parameters influencing the flow resistance in uniform flow. This dimensionless parameter can be defined as follows:

$$\tau_* = \frac{\tau_w}{(\gamma_s - \gamma)d_{50}} \tag{3}$$

[where τ_w is the bed shear stress, γ_s and γ are specific gravity of sediment and water respectively, d_{50} is the median grain size.

Determination of hydraulic parameters

The water surface profile, the curve intersected by the water surface and the longitudinal section, is important in the design of hydraulic structures and river flood control [12]. Hydraulic curve classifications are used to describe the shape of water surface profile at a specific flow. The curves are based on the hydraulic slope (A, H, C, M, or S) and the relative position of the actual flow depth to normal (h_n) and critical (h_c) depths as designated by numbers 1, 2, and 3.

h_n and h_c were calculated with equation 4 and 5. They can analyze the variation of flow state due to vegetated bank.

$$h_c = \sqrt[3]{\frac{Q^2}{gw^2}} \tag{4}$$

$$h_n = \frac{nQ}{wR^{\frac{2}{3}}S_f^{\frac{1}{2}}} \tag{5}$$

Where h_c is the critical flow depth, h_n is the normal depth, n is Manning's coefficient, R is hydraulic radius and S_f is

energy slope.

Using these, we can analyze the variation of flow due to vegetated bank.

Equation 6 calculates the energy dissipation, the total of kinetic energy and potential energy:

$$E = z + h + \alpha \frac{u^2}{2g} \qquad (6)$$

In equation (6) z is the vertical distance of the channel bed from the datum plane and α is the correction factor that equals 1 in the present research.

The turbulence characteristics were also examined by utilizing a normalized quantity TKE defined as:

$$TKE = \frac{1}{2}\rho(\overline{u'^2} + \overline{v'^2} + \overline{w'^2}) \qquad (7)$$

where $u' = u - \bar{u}$, $v' = v - \bar{v}$ and $w' = w - \bar{w}$ are the fluctuations of u, v and w, respectively [10].

The turbulence kinetic energy is an important hydraulic parameter to evaluate the turbulent structure [13]. Turbulence in open channel flow may significantly affect the localized erosion in channel [12]. Actually, the effect of vegetation on turbulent structure depends on multifaceted and interacting factors [14]. Because of the tedious experimental procedures [15], TKE is difficult to experimentally determine.

Shear velocity is one of the factors that directly affect the calculation of resistance coefficient. Thus, the method applied for the calculation is important. This value was estimated by different methods, such as log law (Clauser method), parabolic law, Saint-Venant equation, boundary layer theory, energy gradients, and Reynolds shear stress. In this research, the Saint-Venant equation was used as follows:

$$S_f = S_0 - \frac{dh}{dx}(1 - Fr^2) \qquad (8)$$

$$u_* = \sqrt{ghS_f} \qquad (9)$$

Quadrant analysis

Turbulence is a spatial-temporal process but exhibits regularity. Such coherent motion is called the bursting process. Conditional sampling and statistical techniques are used to detect and characterize the coherent structures. One of the widely used conditional sampling techniques is the quadrant analyses of the Reynolds shear stress [16]. It can be calculated by assessing the contribution of each quadrant to the Reynolds shear stress. Turbulence production can be recognized by quadrant analyses.

The quadrant-hole analysis, first introduced by Lu and Willmarth [17], has been often used to investigate turbulence structures. In this technique, the velocity fluctuations are decomposed into four quadrant domains with the relative quiescent motion excluded from the domain. The first quadrant events (u'>0, w'>0) are "outward interactions", the second quadrant events (u'<0, w'>0), are "ejections", the third quadrant events (u'<0, w'<0) are "inward interactions", and the fourth quadrant events (u'>0, w'<0) are "sweeps" [18].

At any point in steady flow, the contribution to the total

Reynolds shear stress from quadrant i, excluding a hyperbolic hole region of size H, is given by (Yue et al., 2007) [19].

$$D_{H,i} = \frac{1}{T} \int_0^T I_{i,H}[u', w'] dt \qquad (10)$$

where $D_{H,i}$ is the ratio of the number of events at hole sizes exceeding a particular level to the total number of turbulent events.

Drag coefficient

The turbulence due to surface properties, geometric boundaries and other factors cause flow resistance and reduce energy. Thus, the resistance coefficient reflects the dynamic behavior, while flow resistance reduces energy and momentum. The drag coefficient C_d measures the ability of plants to reduce the hydrodynamic force and engineers its own environment [20] and is the key to the success of turbulence models [21].

In most of the literature, the drag coefficient is calculated in terms of submerged vegetation from equation 11:

$$C_d = \frac{2gS}{u^2\lambda} \qquad (11)$$

where g is the acceleration of gravity, S is a water surface slope, λ is the vegetal area coefficient representing the vegetation density per unit channel length (m^{-1}), and h is flow depth. One of the derived empirical relationships that has been presented to calculate the drag coefficient (C_d) due to emergent vegetation is one presented by Cheng (2011) [22]. This relation basically originated from Morison [23] and was modified by Hu et al. (2012). Cheng (2011) proposed a specially defined Reynolds number R_v by using a vegetation-related hydraulic radius r_v as its length scale. This Reynolds number was modified to account for the flow and canopy that vary vertically:

$$R_V = \frac{u \, r_v}{\vartheta} \qquad (12)$$

$$r_v = \frac{1 - \frac{\pi}{4} n \, d^2}{n \, d} \qquad (13)$$

v is the kinematic viscosity, R_V is defined as the ratio of the volume occupied by water per unit area at a certain depth (Δh) to the total frontal area of vegetation per unit area, d is the stem diameter of vegetation and n is the stems density. Since the vegetation Reynolds number R_v varies with flow velocity u and plant characteristic r_v in depth, C_d was modified to be a function of z as well. The original formulation was modified to the following form [21]:

$$C_d = \frac{50}{R_v^{0.43}} + 0.7\left[1 - \exp\left(-\frac{R_v}{15000}\right)\right] \qquad (14)$$

Calculating C_d is difficult for plant structures, because there are interactions between vegetation properties and local hydrodynamic conditions.

Many experimental studies have shown that C_d for vegetation varies greatly with vegetation density, diameter, stiffness as well as the hydrodynamic conditions [22, 24]. Hue et al. (2012) stated that the modified relation depends on local flow conditions and canopy properties in the vertical.

This relation was implemented in an iterative scheme of a 1DVflow model. The modeling results were compared with experimental data of flow through rigid vegetation.

3. Results and Discussion

Effects of vegetation on flow velocity distribution

Flow velocity is an important parameter for evaluating the flow field structure in an open channel flow, especially for non-scouring and non-silting velocities, which affects the soil erosion in rivers [25]. The secondary current can affect the flow structure and change the position of maximum velocity (U_{max}).

Figure 6 shows the velocity distribution for channel and field data, showing that U_{max} occurs under the water surface with and without vegetation on the bank.

Figure 6. Distribution of flow velocity

Some researchers have reasoned that the aspect ratio is an effective factor in creating secondary currents in channels [26]. A small aspect ratio causes a significant impact on the formation of secondary currents in open channels. Using a smooth bed Nezu et al. (1994) [27] and using a gravel bed Graf and Altinakar [28] showed that when the aspect ratio w/h was larger than 5, the secondary currents would not be formed in a channel. This means, when w/h> 5, U_{max} should occur at the water surface [29].

However, our results indicate that U_{max} occurs under water surface for 47 and 34 of all measured profiles, respectively, under flow conditions of channel with w/h = 2.7 and field experiments with w/h = 80. However, the ADV and current-meter are limited for measuring points that have a 5

cm distance from the water surface. This means that one can not definitively comment about profiles that U_{max} is observed at the water surface. The variation of bed slop did not cause any signification change in the position of U_{max}. However near the bank from a central axis (Ax) one can observe that U_{max} occurs downstream. It is intense under the condition of vegetation.

The reason for this change in position of U_{max} is to gather strength of secondary current power by getting closer to the vegetated wall. The dip phenomenon is observed in which U_{max} is below the water surface. Heterogeneity of turbulence is the main factor of the secondary current development. The instant appearance of that shows the occurrence of dip phenomenon. The heterogeneity of turbulence and dip phenomenon are independent of the flow type and they clearly depend on the amount of vorticity and normal and shear stress on the flow.

In this study, under the condition of vegetation on banks and gradually varied flow, the dip phenomenon occurred at 65 % of the water depth. It was at 50% of flow depth for bare bank and at 29 % of flow depth for field data. Therefore, from this study and previous studies it can be concluded that several factors are effective in determining the position of U_{max}, including (1) flow conditions (uniform flow or gradually varied flow), (2) boundary conditions (distance from wall- existence of vegetation or bare bank), (3) vegetation type and density (roughness), (4) aspect ratio, (5) secondary current, and (6) creation of strength vortex (existence of negative velocity value).

Effects of vegetation on water surface profile

The common water surface profiles in the natural waterways are M_1 and M_2. It is expected that vegetation causes to change the flow state, because the flow velocities and water depths along the channel are altered. As shown in figure 7, the water depths, except R-6.5-1.5 % that is M_1, are between the critical and normal water depths in all of the cases. Therefore, the flow state can be determined as gradually varied flow of M_2 type. It is intensified by increasing the bed slope and vegetated bank. For laboratory channel with vegetation on banks, it was observed that the water surface profile changed to fall. Therefore, the variation of water surface profile was an indicator of flow energy dissipation due to the variation of bed slope and the existence of vegetation.

Total energy

The total energy is plotted against y/h in figure 8. As shown in this figure, sections that have vegetation on the bank can increase the total energy in comparing bare bank sections. In these sections the total energy has more variation and dissipation.

Effect of vegetation on turbulent kinetic energy (TKE)

Figure 9 gives the TKE values along the measured sections. The hydraulic condition of gradually varied flow caused the TKE values to decrease for all cases. As can be observed from this figure, for banks with vegetation, the

TKE values were more than for bare banks. In reality the vegetation can increase the turbulence production. The lower TKE values belong to the center axis of channel and the higher values were near wall. This means that the TKE values are related to distance from the side wall.
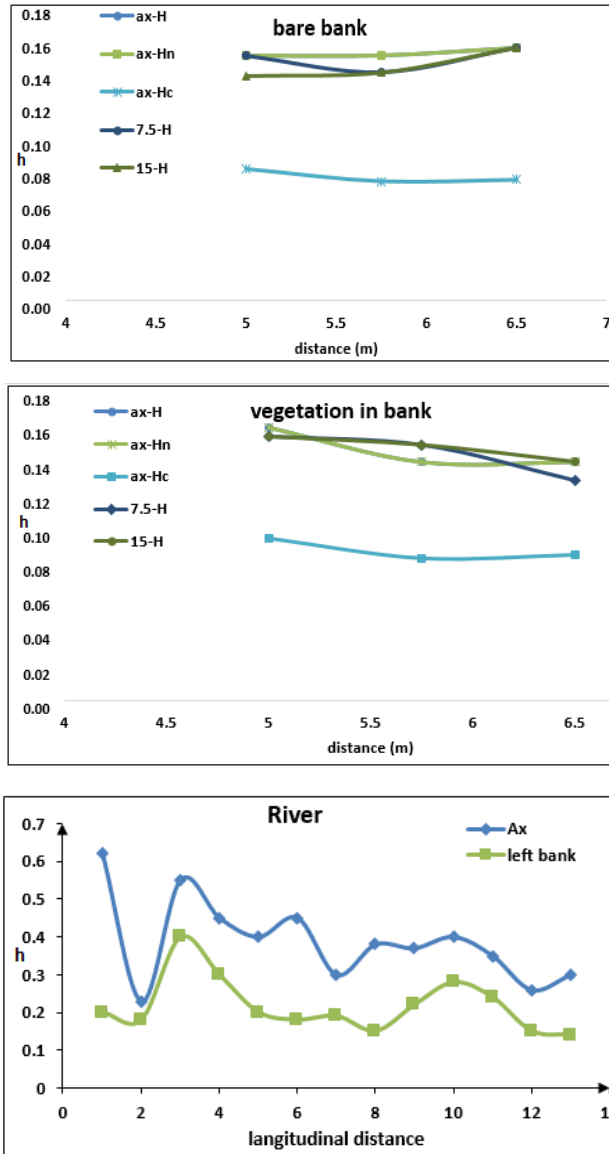

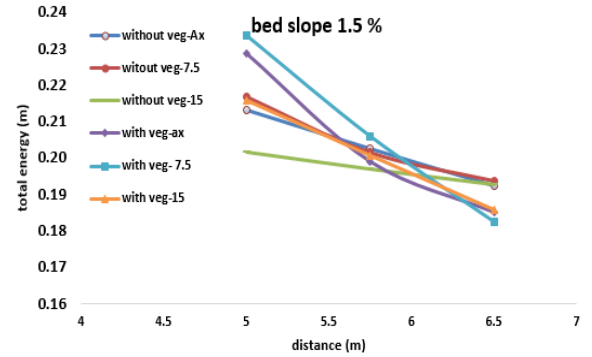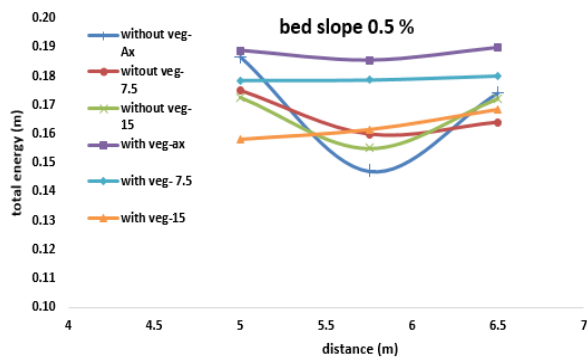**Figure 7.**　Water surface in field and experimental condition

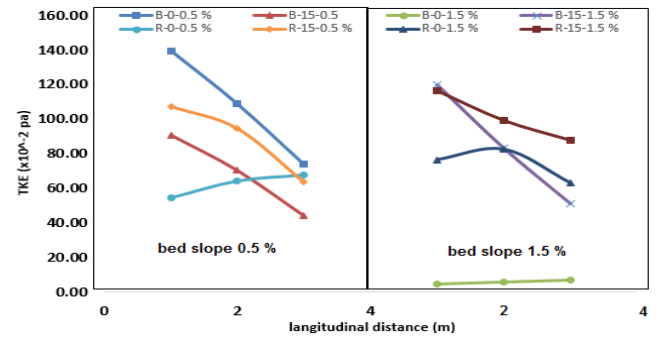**Figure 8.**　Variation of total energy in experimental case

Figure 9.　The TKE values along the measured sections

Distribution of Reynolds's shear stress

Shear stress (-u'w') was dimensionless when divided by the square of velocity obtained through log laws and this parameter was graphed versus $\frac{y}{h}$. The results of the study made on the distribution of dimensionless shear stress, with and without vegetation, are as follows:

1) For the bare bank condition, 18 profiles were studied. In 15 profiles, the amount of shear stress in $0 < \frac{y}{h} < 0.2$ first increased and then from $0.2 < \frac{y}{h} < 1$ showed a decrease. The range of alterations of $\frac{y}{h}$ was between 0.07 and 0.3. In the 3 profiles left, the change in the shear stress was of a decreasing line. The maximum of shear stress was observed near the bed in all these profiles.

2) For the condition of existing vegetation, in 17 cases, the profiles of the distribution of shear stress were in 3 parts:

Part 1: an increase of Reynolds stress near the bed $0 < \frac{y}{h} < 0.14$, part 2: a decrease in Reynolds stress $0.14 < \frac{y}{h} < 0.47$, and part 3: when $0.47 < \frac{y}{h} < 1$ in which the Reynolds shear increased once more. Only in one profile, there was first an increase and then a decrease.

3) With the existence of vegetation, the turning point of the curve moved down and approached the bed. The creation of part 3 of the profiles was also because of the existence of vegetation. It is a bit difficult to realize whether or not there would be part 3 in profiles without vegetation, since the device ADV had some limitations measuring the point 5 cm away from the water surface.

4) Comparing the central axis profiles at -7.5 cm and 5 cm from the wall, we can conclude that the less distance from the vegetation, the more negative figures will appear because of being near the vegetation and the increase in the shear stress level of the momentum absorption. Also the maximum shear stress occurs near the bed.
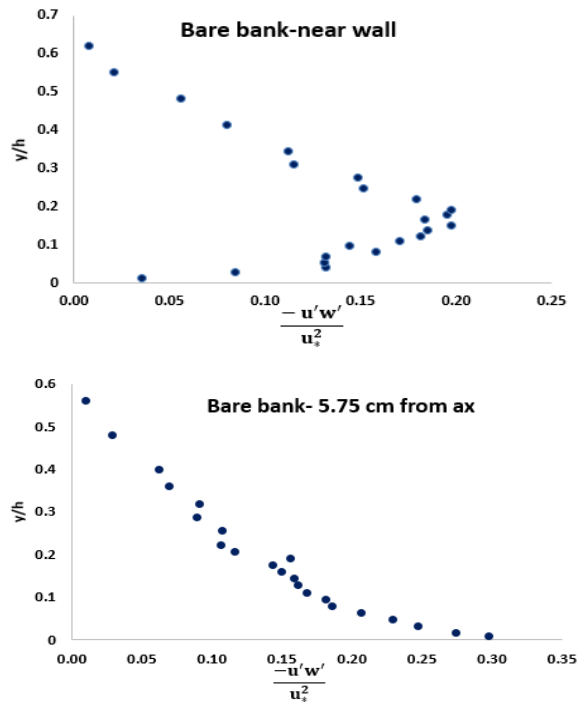
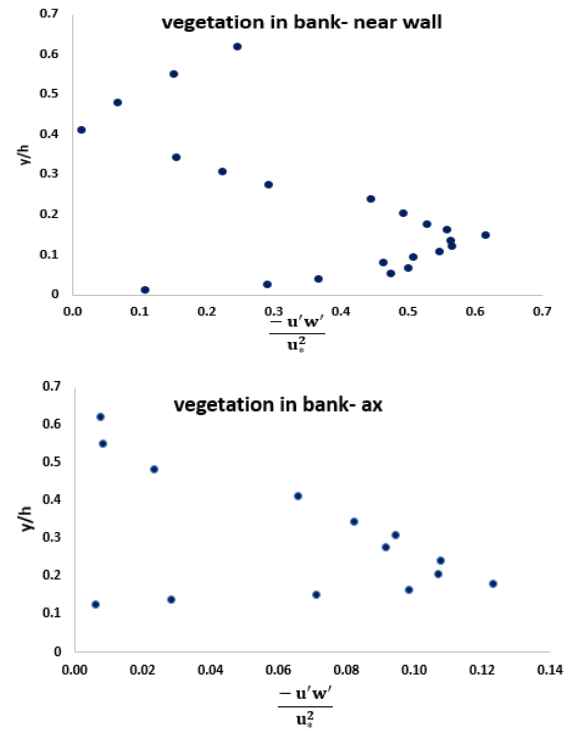**Figure 11.** Distribution of shear stress with vegetation

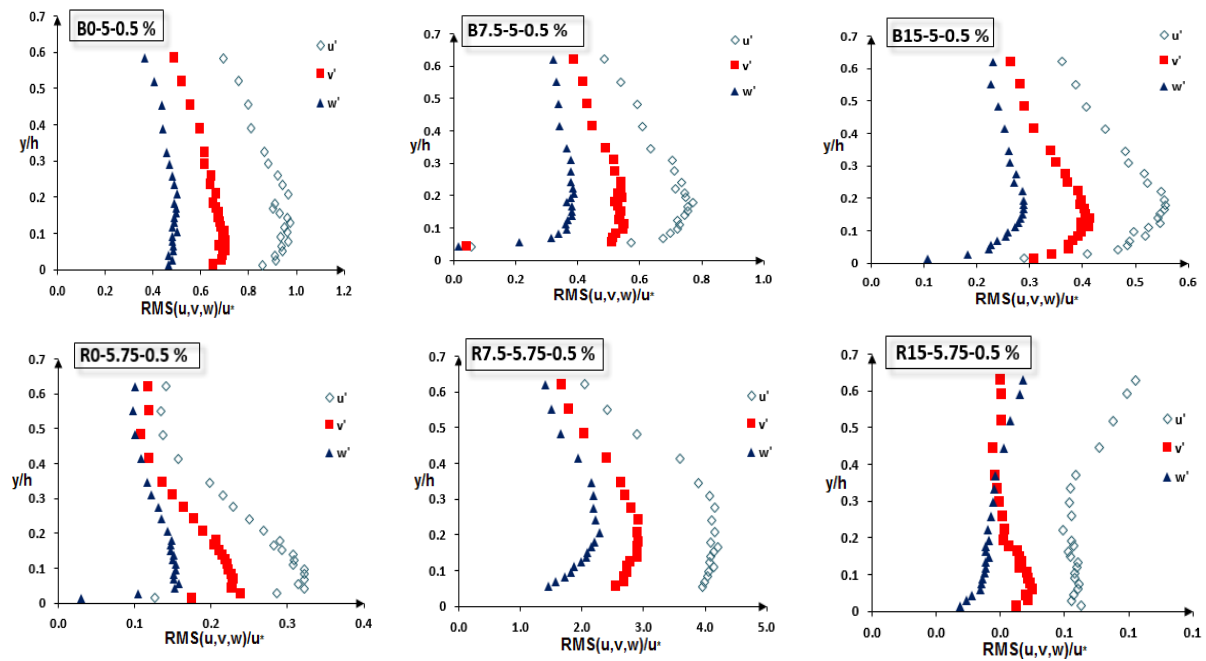**Figure 10.** Distribution of shear stress without vegetation

Figure 12. Sample distribution of RMS (u,v,w)

Turbulence Intensity

Stress tensor components got dimensionless using shear velocity calculated by the Reynolds shear stress method. In all the profiles when there was a bare bank, RMS (u, v, w) was first increasing and then decreasing except for the profile, D15-6.5-1.5% and this occurred in the area $\frac{y}{h} < 0.2$. When there was vegetation, one could observe 3 parts for distributing the velocity turbulence; and the distribution was in accordance with the Reynolds shear stress exactly. The profiles near the central axes displayed more intense curve than that of the walls. Figure 12 shows the sample distribution of RMS (u, v, w).

Quadrant analysis

In this study a program was written in Matlab used to perform quadrant analysis. To perform the quadrant analysis, the amount of the hole parameter was assumed zero (0), meaning that the data contributed to the occurrence of all the dominant processes. Figure 13 shows the dominant turbulent events over the entire flow depth. Considering the bare bank condition, it was observed that at the points near the bed, the largest contribution was for ejection and then sweep. As we got closer to the water surface, the contribution of ejection decreased and that of sweep increased.

The plot of y/h against the contribution of each quadrant can be divided into two regions. The first region with a water depth of 0<y/h<0.45, and the second region with a water depth of 0.45<y/h<1. In the first region, the variation of frequent events (ejection and sweep) was intense. In this region, ejection and then sweep were the most frequent events, while the outward and inward events had small contributions.

In the second region, the variation of contribution was little and the dominant event was sweep and the contribution of outward and inward events increased. It means that events there had a significant role in the region near the water surface. Also, this plot had two regions for condition that had vegetation on bank.

The first region with a water depth 0<y/h<0.35, and the second region with a water depth 0.35<y/h<1. In the first region the dominant event was ejection, followed by sweep, then inward and outward interaction, respectively. In the second region, the contribution of outward and inward interaction increased.

Thus, it can be concluded that in both conditions of with and without vegetation on bank, whenever we got closer to the water surface the distribution of outward and inward interaction increased. It was intensified by vegetation due to the production of turbulence. In agreement with Fazel (2014), it seems that turbulence was much less anisotropic near the vegetated wall compared to that along the center of flume, showing contributions in all four quadrants [16].

Figure 14 shows the contribution of each quadrant to the stress fraction. Similar to figure 13, the plot of y/h against the stress fraction can be divided into two regions. In the bare bank condition, ejection and sweep events had the highest

distribution, but closer to water surface the distribution of their events decreased. In the condition with vegetation compared to bare bank condition, in the second region the distributions of outward and inward events were more than sweep and ejection.
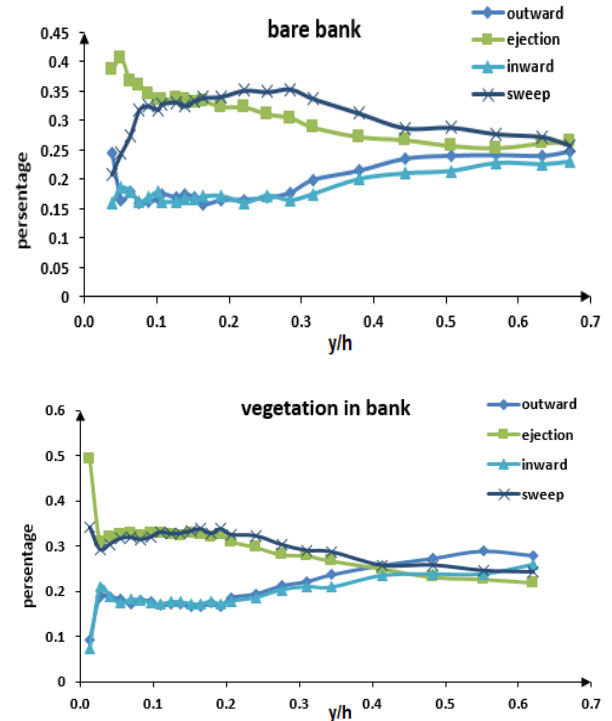

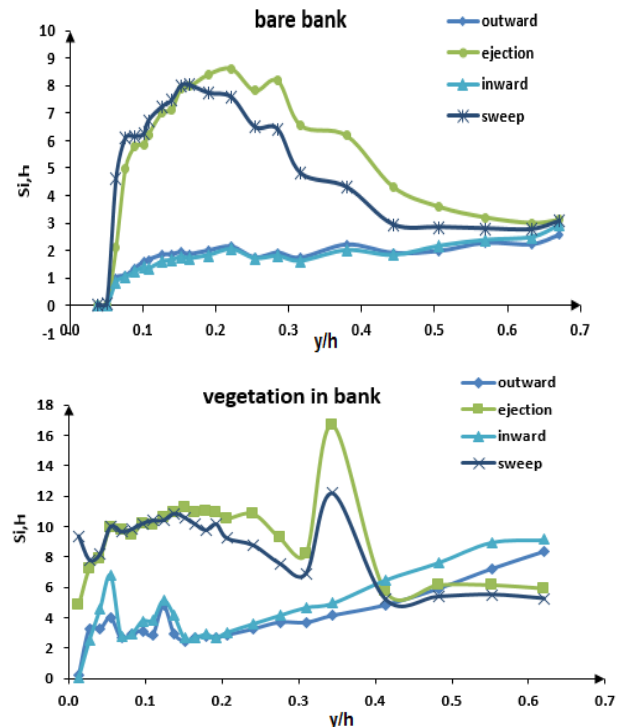**Figure 13.** Dominant turbulent events over the entire flow depth

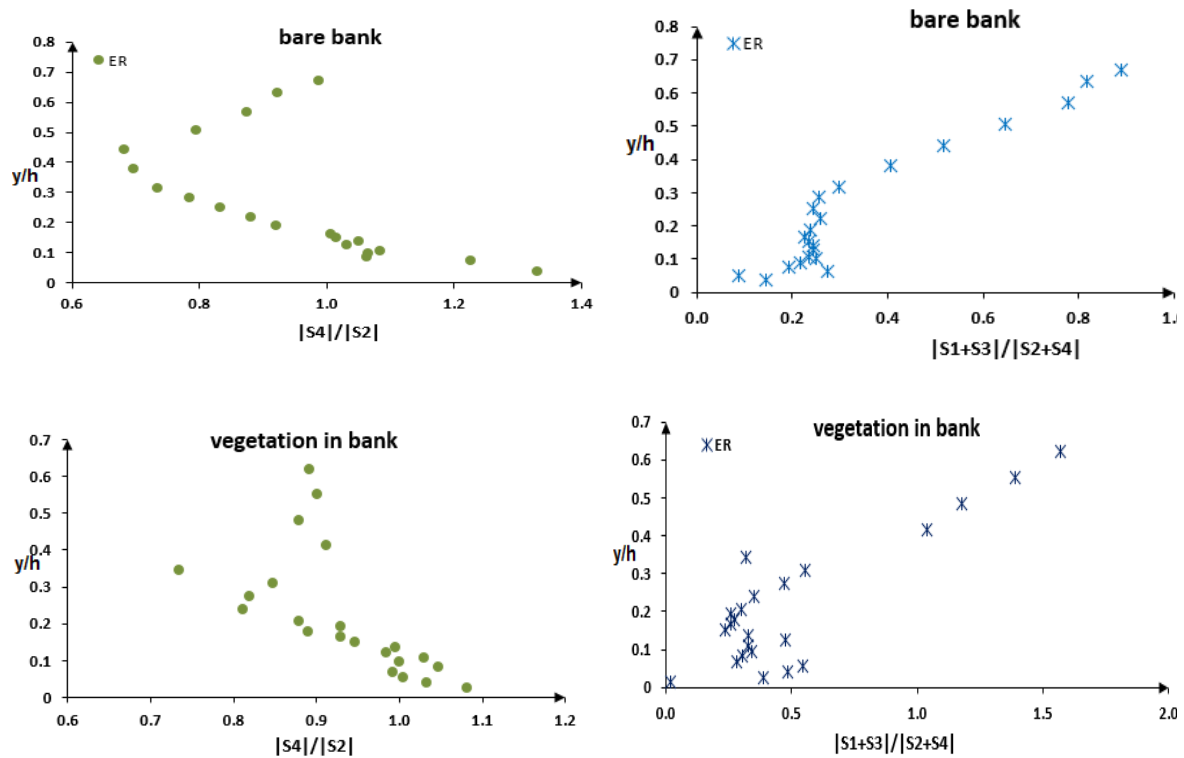**Figure 14.** Contribution of each quadrant to the stress fraction

Figure 15. The ratio of upward and downward components

The ratio of upward and downward components is plotted in figure 15, $|S_{1,H} + S_{3,H)}|/|S_{2,H} + S_{4,H}|$, where $S_{2,H}$ and $S_{4,H}$ are negative, called the exuberance ratio (ER). This ratio is a measurement of the upward momentum transfer against the overall downward flux, showing the exuberant nature of flow. This ratio increases in both cases (with and without vegetation on the bank) from the channel bed towards the water surface.

Under the condition of vegetation on the bank, the intensity of this was more but followed no certain procedure. The existence of vegetation caused the production of flow turbulence as well as the intensity in the exuberance ratio. It is possible to see that in both cases, ER was first increasing ($y/h<0.1$) and then decreasing ($0.1 < y/h<0.2$) and afterward it was increasing ($0.2 < y/h<1$). ER would never be greater than 1 for both cases. The progress of the figure was such that it decreased at first, but from $y/h>0.45$ inclined toward 1 once more.

When there was vegetation this process was first decreasing and then increasing but its amount had fewer or more intensity near 1. It is possible to conclude that vegetation can cause a modification of the proportion of sweep and ejection and an increase in the distribution of outward and inward events.

Quadrant analysis of inflection points of Reynolds stress curve

Inflection points of Reynolds stress curve were the basis for the selection of points for doing this analysis. For the condition of bare bank, the phenomenon of sweep had

occurred both in the canal central axis as well as the near wall with the slope of 5% near the bed and the water surface; therefore, the movement in the flow depths was toward the water surface. While the bed slope was 1.5%, the dominant phenomenon became ejection near the bed. At that point near the bed, the mass and momentum transfer in the flow recurred and moved toward the bed rather than to the surface. Therefore, it can be said that an increase in the slope on the bare bank caused the variation in flow. Table 4 shows the results of quadrant analysis in different experimental series.

On the bare bank, the distance from the wall had no effect on the dominant phenomenon for any of the slopes. When vegetation existed, for the slope of the 5% the dominant phenomenon near the surface and the bed was sweep, while when we approached the wall, the prevailing phenomenon near the bed in the bursting cycle was ejection. Thus, the existence of vegetation on the slope of 5% caused the movement of flow near the bed to tend to the bed. When there was vegetation, an increase in the slope showed that both factors, including the increase in the slope as well as the presence of vegetation raised the turbulence near the bed, and had an impact on the movement of fluid and the turbulence also continued up to the surface. The impact was such that one could not determine a specific process for the change.

In general, the prevailing phenomenon in all studied cases near the surface of water was sweep, except for one which was an outward event, However, at the spots near the bed the percentage of phenomena was as follows: 50% of sweep,

38% of ejection and 12% of inward event. For turning points of the curve, the skewness coefficient versus y/h quadrant analysis was made, as shown in table 5. Studying the third and fourth statistical moments for a channel with vegetation of submerged grass (lawn), Nikora et al (2010) suggested that asymmetrical peaks in the skewness coefficient showed that inside the vegetation the current phenomenon was sweep but was ejection near the crest [30]. In this very study, the turning points of skewness coefficient in profiles near vegetation were in two cases in accordance with what Nikora et al. (2010) found. It is also seen that sweep is the overriding phenomenon near the bed with a slope of 1.5%. In the remainder of profiles, one could not find any certain process in the occurrence of bursting.

Table 4.   Quadrant analysis of inflection points of Reynolds stress curve

Section	Distance from bed (m)	P_1	P_2	P_3	P_4	Dominant Bursting process
B0-6.5-0.5 %	0.024	0.1928	0.303	0.1875	0.3167	Sweep
	0.08	0.1825	0.3017	0.1786	0.3373	Sweep
B0-6.5-1.5 %	0.016	0.1629	0.3508	0.1777	0.3086	Ejection
	0.1	0.2018	0.2912	0.2022	0.3048	Sweep
B15-6.5-0.5 %	0.016	0.1626	0.3222	0.1749	0.3402	Sweep
	0.08	0.2426	0.2531	0.2314	0.2728	Sweep
B15-6.5-1.5 %	0.018	0.1715	0.3344	0.1623	0.3283	Ejection
	0.05	0.1994	0.288	0.1753	0.3373	Sweep
R0-6.5-0.5 %	0.018	0.1937	0.3057	0.1797	0.3209	Sweep
	0.05	0.1973	0.2711	0.1647	0.3669	Sweep
R0-6.5-1.5 %	0.014	0.2724	0.0641	0.4038	0.2579	Inward
	0.04	0.1805	0.3004	0.1785	0.3404	Sweep
R15-6.5-0.5 %	0.01	0.1673	0.3413	0.1885	0.3029	Ejection
	0.05	0.1998	0.2982	0.2026	0.3002	Sweep
R15-6.5-1.5 %	0.022	0.1654	0.3288	0.1726	0.3333	Sweep
	0.06	0.2581	0.2496	0.2347	0.2557	Outward

Table 5.   Quadrant analysis of inflection points of statistical moments

Section	y	P_1	P_2	P_3	P_4	Bursting process
R15- 5- 0.5%	0.123	0.247	0.258	0.209	0.286	Sweep
	0.269	0.279	0.235	0.24	0.247	Outward
R15- 5.75- 0.5 %	0.03	0.191	0.318	0.185	0.306	Ejection
	0.178	0.209	0.294	0.209	0.297	Sweep
R15- 6.5- 0.5 %	0.107	0.176	0.321	0.187	0.316	Ejection
	0.467	0.231	0.275	0.223	0.271	Ejection
R15- 5- 1.5%	0.075	0.156	0.352	0.15	0.343	Ejection
	0.281	0.256	0.257	0.226	0.26	Sweep
R15- 5.75- 1.5 %	0.09	0.194	0.314	0.173	0.32	Sweep
	0.258	0.219	0.281	0.209	0.291	Sweep
R15- 6.5- 1.5 %	0.11	0.169	0.328	0.172	0.331	Sweep
	0.414	0.256	0.247	0.234	0.26	Sweep

Statistics moments

In order to show the influence of vegetation and turbulence, the vertical distribution of normal quantities on the first to fourth statistics moments was evaluated. The study was sequentially temporal and spatially-based.

Temporally-based analysis

In this study the measured velocity data by ADV were 24000 for each point of the profile. To investigate into the temporal basis, the data were divided into six groups of 4000 and statistical moments of 1 to 4 were measured for each group. The time for measuring was selected 120 seconds for each point, thus the time for each group of data was 20 seconds. Figure 16 shows the 1 to 4 statistical moments versus the main group of temporally-based data.

Considering figure 16 (a & b) in relation to the first and second moments, it is plausible to state that these moments for all the profiles in all 6 groups were approximately the same, but the diagrams for the 3rd and 4th statistics moments (c and d) in each group were different and had tolerances in relation to time. Therefore, the first and second moments on a temporally-based basis cannot clearly show the stress alteration and its effect, but the 3rd and 4th moments can clearly show this influence.

When this process was continued for velocity data in the direction of z, as shown in figure 17, it was observed that there were only some tolerances in the first moment in relation to time but the measures were the same for the rest of the moments.
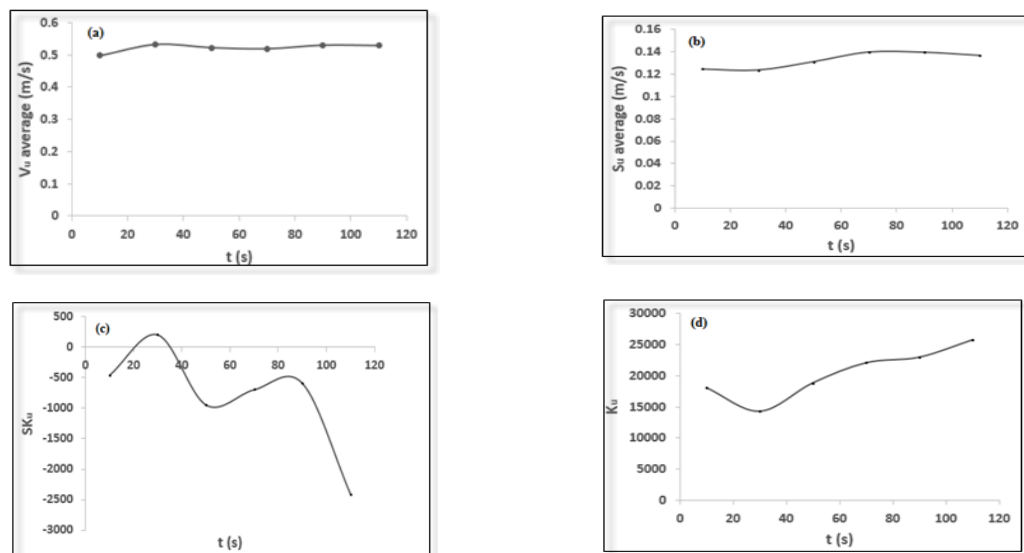

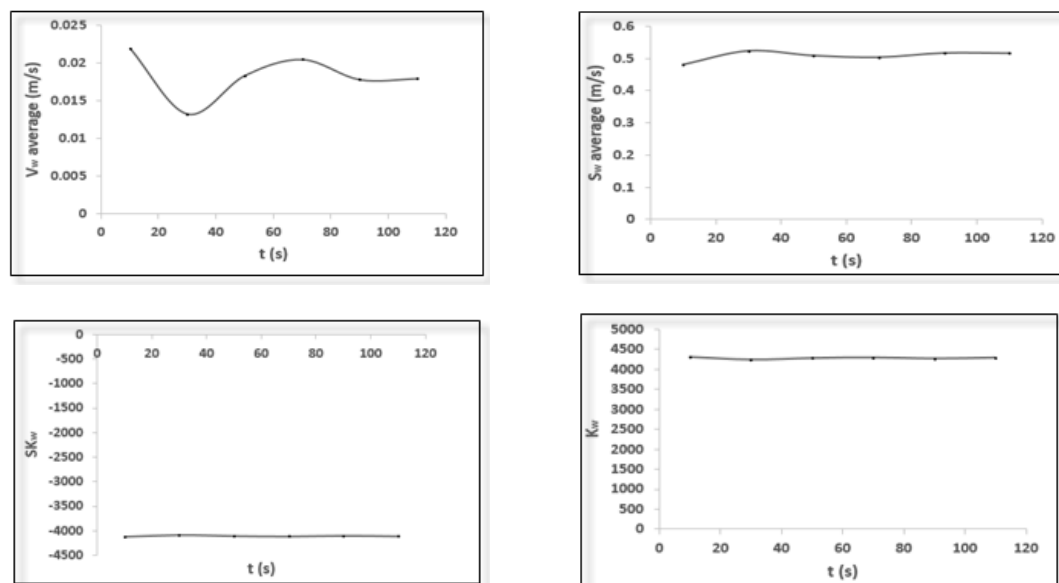**Figure 16.** Statistics moments in the direction of Z

Figure 17. Statistics moments in the direction of Z

Spatially-Based analysis

On a spatially-based basis, the skewness and kurtosis were measured for all the 24000 velocity data. The only difference was that a weighted mean unit in velocity was measured for a whole profile and was used as an average at each point. This was done, because the effect of vegetation and the walls, depending on the position of each point, may vary and if we were to use the average obtained for each point, the so called parameters would affect different points. Through the measurements taken, the influence would not differ for different points. Thereafter, the values of this coefficient versus $\frac{y}{h}$ were drawn as shown in figure 18.

Drag coefficient

The drag coefficient values were calculated by formulas 11 and 14. In calculating this coefficient the shear velocity obtained by different methods was used. Using the Saint-Venant shear velocity in the laboratory experiments, the drag coefficient of equation 7 and 10 to 78% of profiles

was different, less than ±30%, as shown in Figure 19.

The rest of computational methods of shear velocity in the laboratory and field did yield similar values. By plotting y/h against C_d calculated from equation 14 it can be observed that in all experimental cases, C_d increased when the water surface decreased. For up to y/h =0.1 the variation of C_d was intense and its value was greater than 1. But for y/h>0.1 this coefficient was in the range of 0.85 to 1. The existence of vegetation caused that the variation of Cd reduced and it created a much closer graph. The C_d calculated from equation 11 had a similar pattern for both field and experimental conditions and it was in the range of 0.82 to 1.06, whereas field data had more change. What is clear is that when using equation 11 for calculating C_d, its values were between 0.29 and 0.8 for the laboratory channel, and it was between 0.038 and 0.97 for field experiments. Therefore, it seemed that the variation of calculating C_d considered more hydraulic parameters of low.
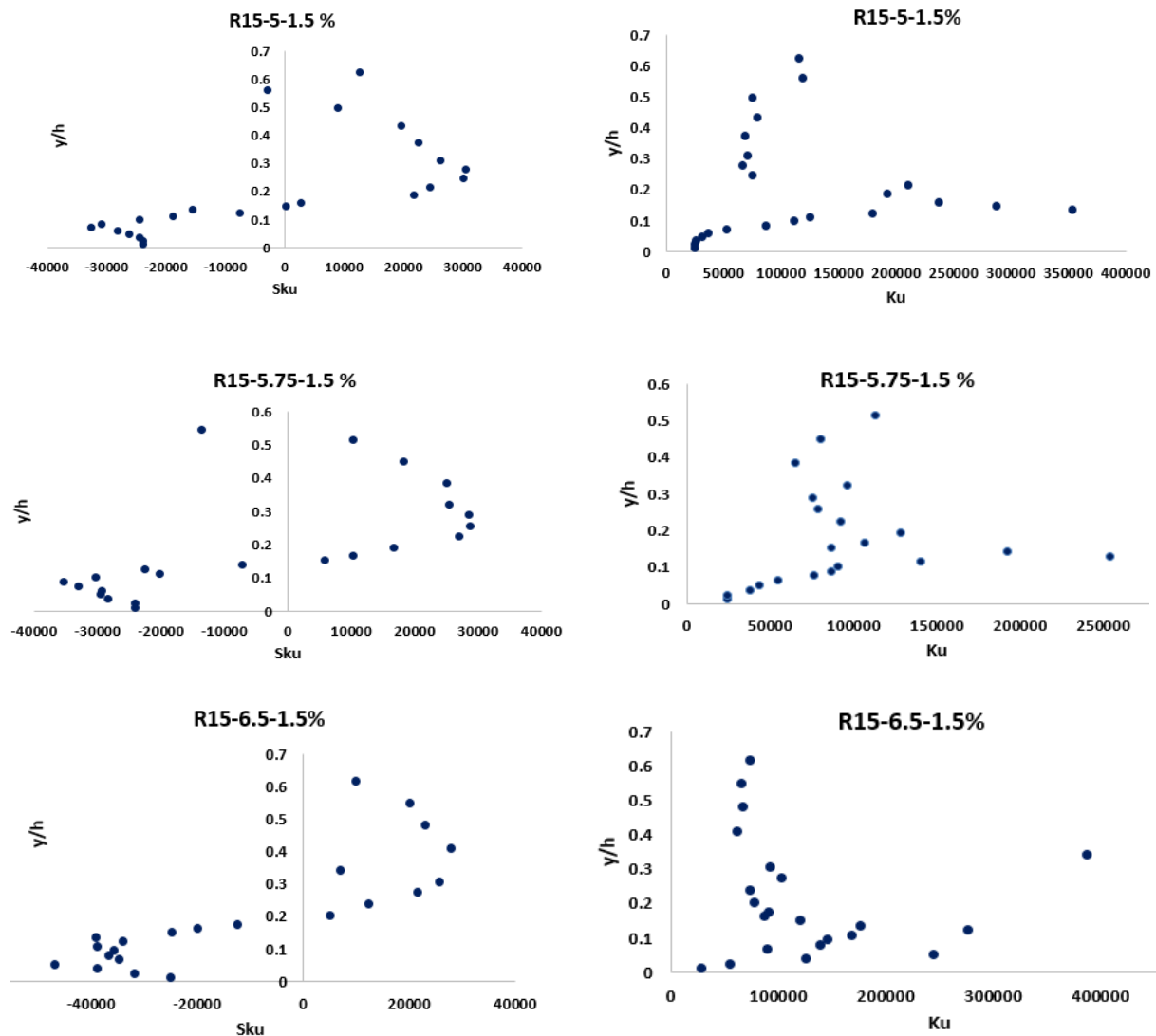

Figure 18.   A sample of the 3rd and 4th statistical moment with vegetation in spatially–based form
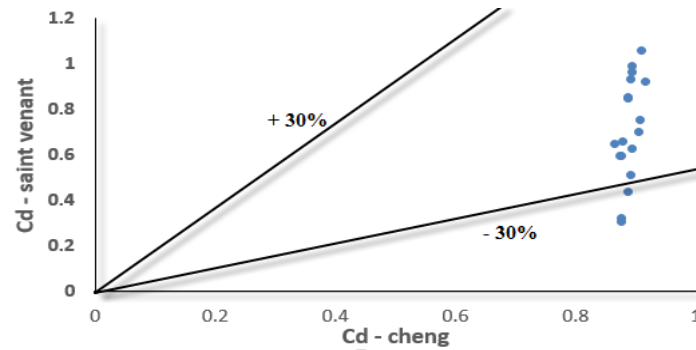
Figure 19. Comparison of Drag Coefficient Calculated by Equations 7 and 10

Relation between drag coefficient and dimensionless parameter

Froude number

Figure 20 shows a plot C_d against Froude number (Fr). For all of the laboratory experiments, the relation between C_d and Fr was a regular exponential decline with $R^2 > 0.95$. The existence of vegetation and the increase in bed slope increased the variation of C_d. For field experiments, for Fr>0.45 the variation of C_d inclined towards a constant amount.
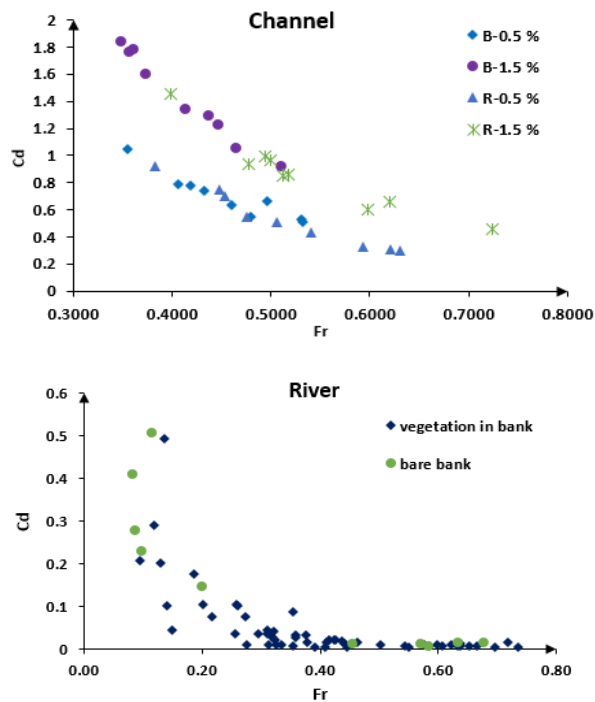

Figure 20. The relation between Froude number and C_d

Reynolds number

Considering figure 21, it is possible to get to similar results for the relation between C_d and Re.

For the field data, for Re>1.5×10^5 the variation of C_d inclined towards a constant value. When the aspect ratio is plotted against the variation of C_d, it can clearly be identified

that with the increase in the aspect ratio, the variation of C_d increased first and then decreased.
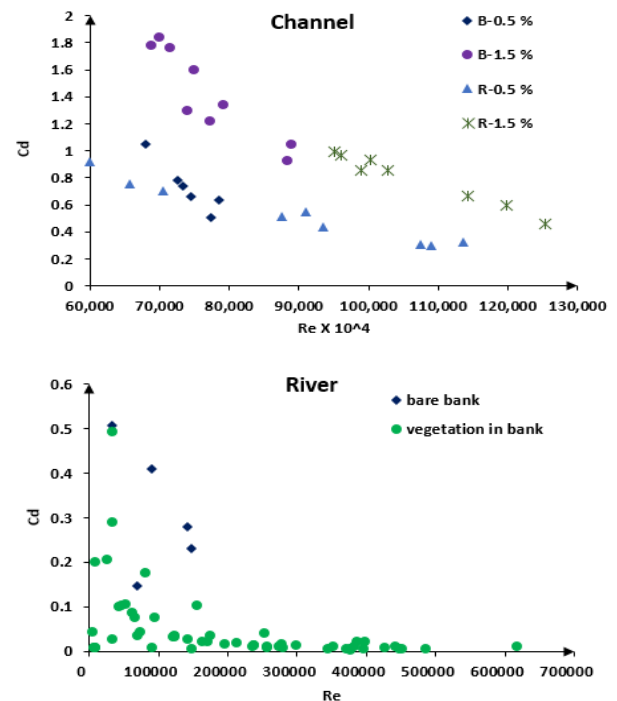

Figure 21. The relation between Reynolds number and C_d

Aspect ratio

The aspect ratio is one of the main factors belonging to the secondary current type 2 due to turbulence inhomogeneities. The existence of vegetation on banks and the aspect ratio 2.7 in laboratory experiments contributed remarkably to the vorticity gradient and led to an increase in the variation of C_d (figure 22). That is why C_d in laboratory experiments was greater than for field data with an aspect ratio of 80.

Shields parameter

As shown in figure 23 for laboratory experiments, C_d and Shields parameter had a linear relation, which means that an increase in Shields parameter produced an increase in C_d. For field data, no meaningful relation was witnessed between these two.
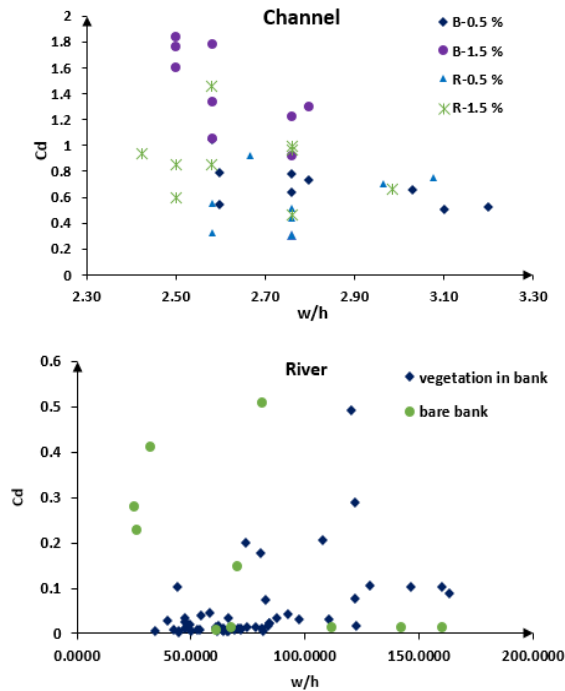
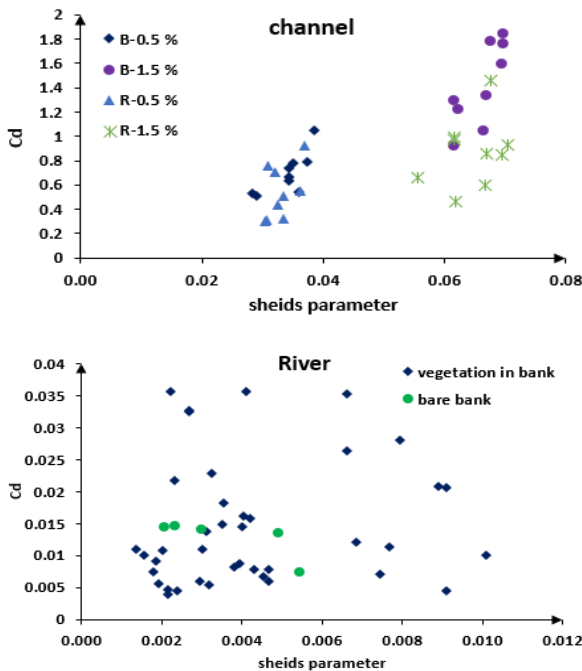**Figure 22.**   The relation between aspect ratio and C_d

Figure 23.   The relation between C_d and shields parameter

4. Conclusions

The following conclusions are drawn from this study:

(1) U_{max} occurs under the water surface with and without vegetation on the bank. It occurs under water surface for 47 and 34 percent of all measured profiles, respectively, under flow conditions of channel with w/h = 2.7 and field experiments with w/h = 80.

(2) Under the condition of vegetation on banks and gradually varied flow, the dip phenomenon occurred at 65% of the water depth. It was at 50% of flow depth for bare banks and at 29% of flow depth for field data.

(3) The total kinetic energy (TKE) values were more for banks with vegetation than for bare banks. The lower TKE values belong to the center axis of channel and the higher values are for near wall.

(4) For vegetation, the distribution of shear stress contained 3 parts: Part 1: an increase of Reynolds stress near the bed $0 < \frac{y}{h} < 0.14$, part 2: a decrease in Reynolds stress $0.14 < \frac{y}{h} < 0.47$, and part 3: when $0.47 < \frac{y}{h} < 1$ in which the Reynolds shear increased once more.

(5) Turbulence was much less anisotropic near the vegetated wall compared to that along the center of flume.

(6) Vegetation reduced the variation of drag coefficient.

(7) For laboratory experiments, the relation between C_d and Fr was an exponential decline. Vegetation and an increase in bed slope increased the variation of C_d. For field experiments, for Fr>0.45 the variation of C_d inclined towards a constant amount.

(8) Drag coefficient (C_d) for small aspect ratio (laboratory run) is greater than large aspect ratios (field runs). Also, there is a direct relation between C_d and Shields parameter for small aspect ratios, while no relation was observed for large aspect ratios.

Notation

h	Flow depth (m)
u	Main flow velocity (m/s)
U_{max}	Maximum velocity (m/s)
w	Channel width (m)
w/h	Aspect ratio
R	Hydraulic radius (m)
Q	Flow discharge (m³/s)
Re	Reynolds number
Fr	Froude number
S_f	Energy slope
ρ	Fluid density
g	Gravitational acceleration
λ	Vegetal area coefficient
μ	Dynamic viscosity (pa.s)
τ_*	Shields parameter
τ_w	Wall shear stress
h_n	Normal depth (m)
h_c	Critical depth (m)
z	Vertical distance of the channel bed
α	Correction factor
TKE	Turbulence kinetic energy
S_0	Bed slope
u_*	Shear velocity
C_d	Drag coefficient
ν	Kinematic viscosity (m²s⁻¹)
r_v	Vegetation-based hydraulic radius

| d | Vegetation diameter (m) |
| N | Total number of plants in control volume |

REFERENCES

[1] Kemp J. L., Harper D. M. and Crosa G. A., 2000, The habitat-scale eco-hydraulics of rivers. Ecol Eng; 16(1):17–29.

[2] Costanza R, d'Arge R. and de Groot R, et al., 1998, The value of the world's ecosystem services and natural capital. Ecol Econ; 25(1):3–15.

[3] Tang HW, Lv SQ, Yan J and Zhou YL, et al., 2008, Water environment improvements in Zhenjiang city, China. Proc Inst Civil Eng-Munic; 161(1): 11–6.

[4] Kouwen, N. and M. Fathi-Moghadam, 1997, Non-rigid, non-submerged, vegetative roughness on floodplain, J. Hydraul. Eng. 1:51-57.

[5] White, B. L. and H. N. Nepf, 2007, A vortex-based model of velocity and shear stress in a partially vegetated shallow channel, Water Resour. Res. 44: W01412-WR005651.

[6] David, L., 2008, Flow through Rigid Vegetation Hydrodynamics, Thesis of Master of Science, Virginia Polytechnic Institute and State University.

[7] Callow J. N., 2012, Potential for vegetation-based river management in dryland, saline catchments. River Research and Applications28(8:(1072–1092. DOI: 10.1002/rra.1506.

[8] experimental study, 2013.

[9] Fu-Sheng, W., W. Wen-Ye and J. Shu-Hai, 2007, Hydrodynamics development in vegetated open channel Shuikexue Jinzhan. Advances in Water Science. 18(3): 456-461.

[10] Colosimo, O., V. A. Copertino and M. Veltri, 1988, Friction factor evaluation in gravel-bed Rivers. J. Hydr. Eng. ASCE. 114(8): 861-876.

[11] Afzalimehr, H. and F. Anctil, 1998, Estimation of Gravel Bed River Flow Resistance. J. Hydraul. Eng. 10: 1054-1058.

[12] Zhang H. Y., Wang Z. Y., Xu W. G. and Dai L. M., 2014, Effects of rigid unsubmerged vegetation on flow field structure and turbulent kinetic energy of gradually varied flow, River research and applications.

[13] Yagci O, Tschiesche U, Kabdasli MS, 2010, The role of different forms of natural riparian vegetation on turbulence and kinetic energy characteristics, Advances in Water Resources 33(5): 601–614. DOI: 10.1016/j. advwatres.2010. 03.008.

[14] McBride M, Hession WC, Rizzo DM. and Thompson DM., 2007, The influence of riparian vegetation on near-bank turbulence: a flume experiment.

[15] López F. and García M., 2001, Meanflow and turbulence structure of openchannel flow through non-emergent

[16] Fazel E. N., Afzalimehr H. and Sui J., 2015, Turbulent characteristics of favorable pressure gradient flow in gravel-bed channel with vegetated walls, J. Hydrol. Hydromech.

[17] Lu, S., and W. W. Willmarth, 1973, Measurements of the structure of the Reynolds stress in a turbulent boundary layer, J. Fluid Mech., 60, 481– 511.

[18] Yue W., Meneveau C., Parlange M., Zhue W. and Hout R., 2007, A comparative quadrant analysis of turbulence in a plant canopy water resource research.

[19] Yue, W., Meneveau, C., Parlange, M.B., Zhu, W., Hout, R.V. and Katz, J., 2007, A comparative quadrant analysis of turbulence in a plant canopy. Water Resour. Res., 43, W05422.

[20] Bouma, T. J., M. B. De Vries, and P. M. J. Herman, 2010, Comparing ecosystem engineering efficiency of two plant species with contrasting growth strategies ,Ecology, 91(9), 2696–2704.

[21] Hu, Z., Stive, M., Zitman, T. and Suzuki, T. 2012, Drag coefficient of vegetation in flow modeling .Proc. 33rd Int. Conf. on Coastal Engineering, Santander, Spain

[22] Cheng, N., 2011, Hydraulic radius for evaluating resistance induced by simulated emergent vegetation in open-channel flows. Journal of Hydraulic Engineering, 137 (9), pp. 995–1004.

[23] Nehal L., Hamimed A. and Khaldi A., 2013, Experimental study on the impact of emergent vegetation on flow.

[24] Tanino, Y. & Nepf, H., 2008, Laboratory investigation of mean drag in a random array of rigid ,emergent cylinders, Journal of Hydraulic Engineering, 134 (1), pp. 34–41.

[25] Tang W, Zhang HY, Huang TS. and Dai LM, 2012, The dynamical relationship between vegetation and sediment in arid and semiarid areas, Journal of Applied Nonlinear Dynamics1: 263–277.

[26] Sui J., Faruque M. A. A., and Balachandar R., 2008, Influence of channel width and tailwater depth on local scour caused by square jets, Journal of Hydro-environment Research (Elsevier Science), Vol. 2, pp. 39–45.

[27] Nezo, I. and Nakagava H., 1994, Turbulence in open channel flow. J. Fluid. Mech. 269: 373-374.

[28] Graf W. H. and Altinakar M. S., 1998, Fluvial Hydraulics: Flow and Transport Processes in Channels of Simple Geometry. Wiley: New York.

[29] Afzalimehr H., Sui J. and Moghbel R., 2010, Hydraulic parameters in channel with wall vegetation and gravel-bed. International Journal of Sediment Research.

[30] Nikora, V., 2010, Hydrodynamics of aquatic ecosystems: An interface between ecology, biomechanics and environmental fluid mechanics. River Res. Applic.26 (4): 367–384.

vegetation. Journal of Hydraulic Engineering 127(5): 392–402. DOI: 10.1061/(ASCE)0733-9429(2001)(127% 3A5(392).